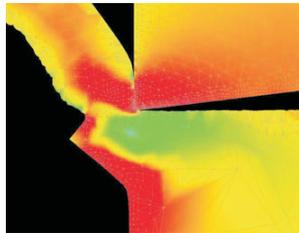**Fraunhofer** Institut
Werkzeugmaschinen
und Umformtechnik

8th CIRP International Workshop on Modeling of Machining Operations

May 10-11, 2005
Chemnitz, Germany

Proceedings

The Role of the Relative Tool Sharpness in Modelling of the Cutting Process

J. C. Outeiro[1] and V. P. Astakhov[2]

[1] Graduate School of Science and Technology, Portuguese Catholic University,
3080-032 Figueira da Foz, Portugal.

[2] Astakhov Tool Service, 3319 Fulham Dr., Rochester Hills, MI 48309, USA.

Abstract

Although the definition of the cutting tool edge radius is self-evident, its influence on the cutting process is ambiguous. Therefore, a certain qualitative assessment criterion should be developed to classify the cutting edge as to be sharp or rounded in the modelling of the cutting process. It is particularly important because carbide insert manufacturers supply the same product with different radii of the cutting edge.

This paper quantifies the importance of the cutting edge radius. It considers the ratio of the cutting edge radius and the uncut chip thickness as the relative sharpness of the cutting edge (RTS). The influence of RTS on the cutting process was analyzed analytically, numerically and experimentally. The paper discusses the influence of RTS on the energy flows in the metal cutting system and the energy balance of this system.

1 INTRODUCTION

Although the definition of cutting tool edge radius is self-evident, it is more difficult to assess the influence of this parameter on the cutting process and thus to classify the tool cutting edge as to be sharp or rounded. This is because the sharpness is a relative parameter, which depends on the ratio of the tool cutting edge radius and the uncut chip thickness. Even if the cutting tool edge radius is small, it may have a significant influence on the cutting process if the uncut chip thickness is of the same order or even smaller than the cutting tool edge radius. Zorev [1] suggested the following empirical rule: the radius of the cutting edge does not affect the cutting process if this radius equal or less than 1/10 of the uncut chip thickness. In many practical machining operations, however, this ratio exceeds 1/10. As a result, the radius of the cutting edge should be considered as a significant factor in the modelling the cutting process. For example, if one tries to evaluate the influence of the cutting feed and the parameters of the cutting tool geometry that might affect on the cutting process, the discussed 1/10 ratio should be always kept in mind.

2 THE ROLE OF THE TOOL CUTTING EDGE RADIUS ON CUTTING PROCESS

2.1 Definition of Relative Tool Sharpness

In general, both cutting tool edge radius and the uncut chip thickness (mainly affected by the cutting feed) may vary and thus the previous considerations lead to the introduction, of a criterion referred to as the Relative Tool Sharpness (hereafter, RTS) of the cutting edge, and defined by the following equation,

$$RTS = \frac{a_r}{r_n} \qquad (1)$$

where a_r is the uncut chip thickness and r_n is the radius of the cutting edge.

The maximum value of this ratio that corresponds to negligibly small influence of the cutting edge radius on the cutting process is referred to as the critical relative tool sharpness $RTS_{critical}$.

Due to the finite radius of the cutting tool, ploughing occurs in every metal cutting process [2,3]. As RTS increases, ploughing competes directly with cutting. In this work is assumed that the total uncut chip thickness, a_r, is separated into the actual uncut chip thickness,

a_1, and the layer to be burnished, h_p, by the round part adjacent to the tool flank face.
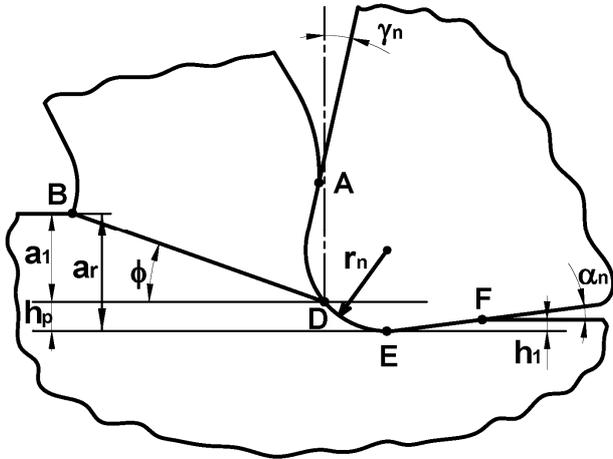

Figure 1: Model of the rounded tool cutting edge.

2.2 Influence of RTS on cutting geometry

Because the actual uncut chip thickness, a_1, is smaller than the total uncut chip thickness, a_r, the cutting feed corresponding to the actual uncut chip thickness can be thought of as the apparent cutting feed, f_1 which is smaller that the real cutting feed, f measured as the velocity of tool along the workpiece as shown in Figure 2. As seen, the apparent cutting feed, f_1 can be calculated as

$$f_1 = \frac{a_1}{\sin(\kappa_r)} = f - \frac{h_p}{\sin(\kappa_r)} \qquad (2)$$

where κ_r is the tool cutting edge angle.

This equation is valid when $a_r > h_p$, or, as it

follows from Eq. (2), when $f > \dfrac{h_p}{\sin(\kappa_r)}$ (to

keep $f_1 > 0$).

The use of small RTS' also induces changes in the actual or corrected tool rake angle. We suggest the following method (referred to as the method of tangent) to calculate this rake angle using a model shown in Figure 3.

In this figure, the corrected normal rake angle, γ_n', corresponds to the angle between the trace of the reference pane (the vertical direction in Figure 3) and the tangent to the rake face profile at point A that corresponds to a_r as shown in Figure 3.

According to the method of tangent, the actual rake angle calculates as

$$\gamma_n' = \begin{cases} \arcsin\left(\dfrac{a_r}{r_n} - 1 \right) & if \quad a_r < r_n \cdot \left(1 + \sin\gamma_n\right) \\[2mm] \gamma_n & if \quad a_r \geq r_n \cdot \left(1 + \sin\gamma_n\right) \end{cases}$$

$$(3)$$

where γ_n is the normal tool rake angle.

It is understood that the actual rake angle given by Eq. (3) characterizes the rake angle only in one point and thus cannot represent the actual geometry of the rounded rake face because the rake angle varies over the rounded part of the cutting edge.

To improve the determination of the corrected normal rake angle, another method referred to as "Method of Incremental Rake Angle" was developed. As shown in Figure 4, this method consider the division of the uncut chip thickness, a_1, into small elementary layers each having thickness Δa_1. The corrected rake angle is then calculated for each layer as

$$\gamma_{n,i}' = \begin{cases} \arcsin\left(\dfrac{a_{ri}}{r_n} - 1 \right) & if \quad a_{ri} < r_n \cdot \left(1 + \sin\gamma_n\right) \\[2mm] \gamma_n & if \quad a_{ri} \geq r_n \cdot \left(1 + \sin\gamma_n\right) \end{cases}$$

$$(4)$$

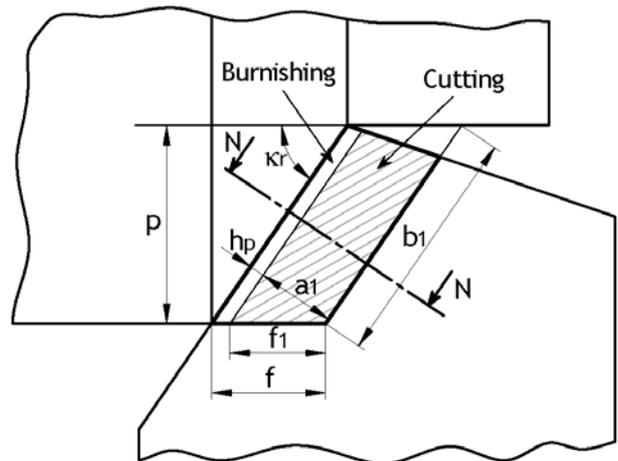where $a_{r_i} = a_{r_{i-1}} + \Delta a_{r_i}$.

Figure 2: Schematic representation of the corrected feed due to the cutting tool edge radius effect.
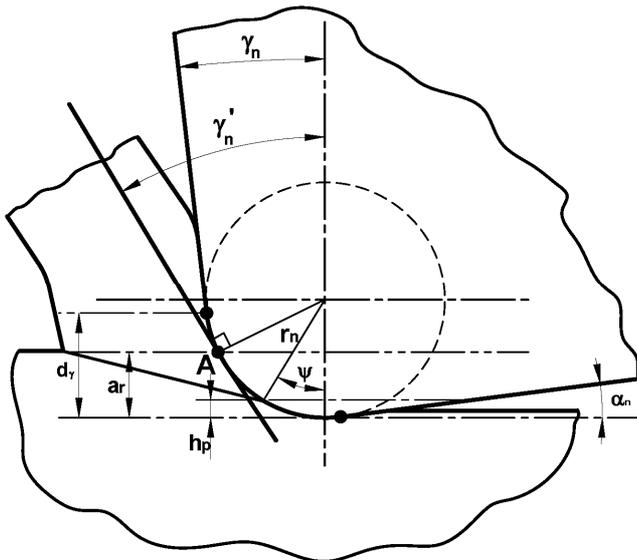
Figure 3: Model for determination of the corrected tool rake angle, using the method of the tangent.
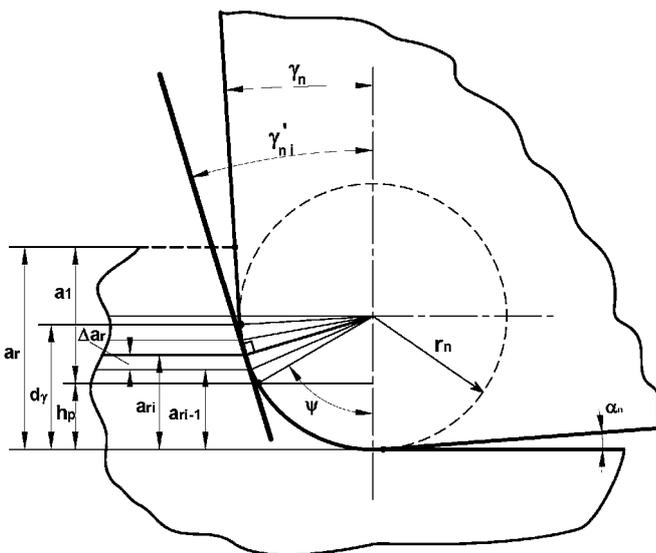

Figure 4: Model for determination of the corrected tool rake angle, using the method of incremental rake angle.

3 ANALYTICAL APPROACH

Figure 5 shows the flowchart of the proposed analytical approach to study the influence of RTS on the temperatures and thermal energy distributions in the deformation zone. A detailed description of this approach can be found in [4]. This analytical approach can be applied to any practical (three-dimensional) metal cutting operation.

The analytical approach includes three main steps:

1. Determination of the corrected feed, f_1, and the corrected normal rake angle, $\gamma_n^{'}$, due to the cutting tool edge radius effect, using the procedures described in the previous Section.

2. Determination of the equivalent cutting geometry. To make analytical studies of three-dimensional cutting process easier, some simplification of the real cutting process are needed. One of the common simplifications is the introduction of the concept of the equivalent cutting edge. This cutting edge replaces the major and minor cutting edges in the manner shown in Figure 6 [4-7]. This equivalent cutting edge is defined as a straight line that connects the end of the major and minor cutting edges as shown in Figure 6. Ones the equivalent cutting edge is constructed, the direction of chip flow is assumed to be perpendicular to this edge. As any cutting edge, this edge is characterized by the equivalent geometry including a set of equivalent angles: tool rake angle, γ_e^{eq}, tool flank angle, α_e^{eq}, tool inclination angle, λ_s^{eq}, and tool cutting edge angle, κ_r^{eq}. Adopting these simplifications, 3D cutting can be represented by orthogonal cutting so orthogonal cutting theory can be applied to estimate the forces and temperatures generated in three-dimensional cutting process. In turn, the determination of the equivalent cutting geometry includes three steps:

   i. Determination of the chip flow angle, η_c, using the Colwell model (Figure 6).

   ii. Determination of the equivalent cutting edge geometry $(\gamma_e^{eq}, \alpha_e^{eq}, \lambda_s^{eq}, \kappa_r^{eq})$.

   iii. Determination of the uncut chip cross-section area as the product of the true uncut chip width, b_{1T} and true uncut chip thickness, a_{1T} in the manner as suggested by Klushin [8]. The detailed methodology of determination of b_{1T} and a_{1T} is describes in details by Astakhov [9].

3. The equivalent cutting geometry together with other input parameters such as cutting speed, feed, physical and mechanical properties of the work and tool materials, geometry of the

workpiece are used to calculate the relevant similarity numbers [9,10]. Then the analytical model for the orthogonal cutting is employed to predict the temperatures and thermal energy distribution in the deformation zone [9,10] (the output parameters).

4 PREDICTED AND EXPERIMENTAL RESULTS

4.1 Experimental setup and parameters

Turning tests were carried out using a 35 kW numerically controlled lathe equipped with a specially designed experimental setup. This experimental setup included thermal imaging equipment developed to assess the
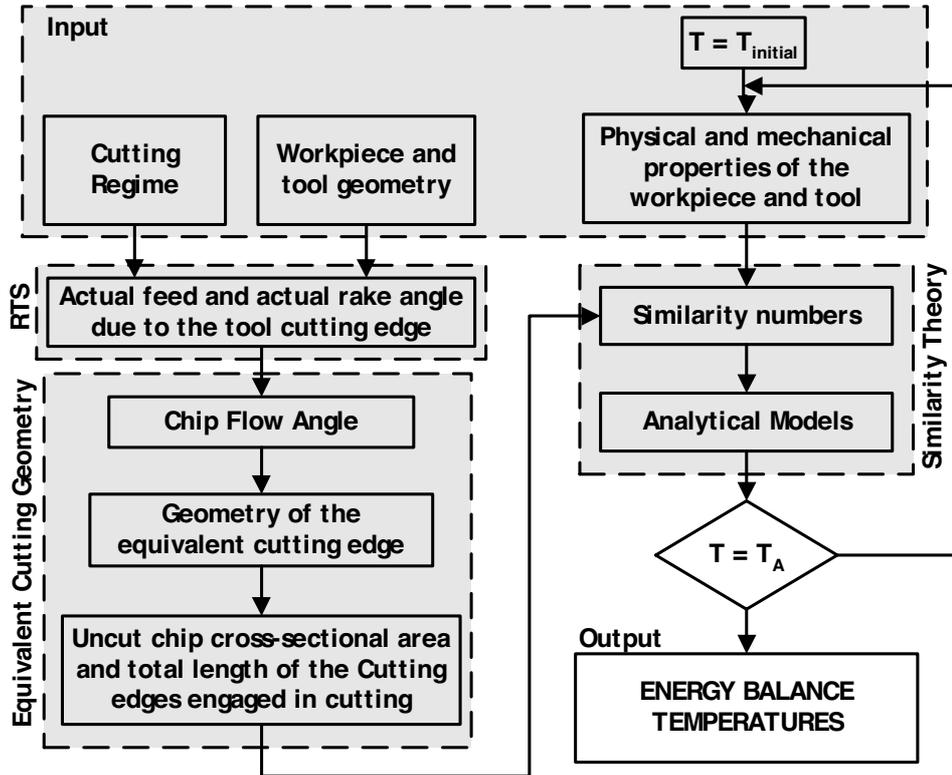

Figure 5: Flowchart of the analytical approach used in the prediction of the temperatures and thermal energy distribution in the deformation zone.
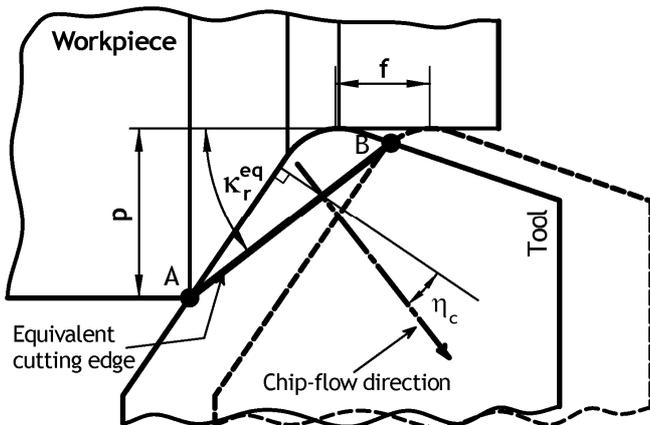

Figure 6: Definition of equivalent cutting edge using Colwell rule.

temperature distribution in the deformation zone in three-dimensional cutting. A detailed description of this equipment and its calibration can be found in [11].

A brief description of the selected levels of each parameter used in the tests is given in the following lines:

Work material. Round bars (140 mm in diameter) of AISI 1045 steel and AISI 316L steel were selected for this study.

The physical parameters of the AISI 1045 steel are temperature dependant and given by the following equations [12,13]: density, $\rho_w(T) = 7933.3 - 0.2805 \cdot T$ (Kg/m^3); specific heat, $c_{p,w}(T) = 467.88 + 0.1888 \cdot T + 0.0006 \cdot T^2$ (J/KgK); thermal conductivity, $k_w(T) = 40.641 - 0.0096 \cdot T$ (W/mK). For the AISI 316L the physical parameters are given by following equations [14]: density, $\rho_w(T) = 7921 - 0.614 \cdot T + 0.0002 \cdot T^2$ (Kg/m^3);

specific heat,
$$c_{p,w}(T) = 440.79 + 0.5807 \cdot T - 0.001 \cdot T^2 + 7 \times 10^{-7} \cdot T^3$$
(J/KgK); thermal conductivity,
$$k_w(T) = 14.307 + 0.0181 \cdot T - 6 \times 10^{-6} \cdot T^2 \text{ (W/mK)}.$$

Cutting tool. Both uncoated (ISO M10-M20/K05-K15) and coated (ISO P25-P45) tungsten carbide inserts were selected for the present study. The coated inserts were with CVD triple layer (TiC/TiCN/TiN). Except for the tool cutting edge radius, the other tool geometry parameters were the same for both kind of tools as follows: normal rake angle, γ_n = -4.29°; normal relief (flank) angle, α_o = 4.29°; normal wedge angle, β_o = 90°; inclination angle of the cutting edge, λ_s = -14°; tool cutting edge angle, κ_r = 72°; nose radius, r_ε = 0.8 mm. The tool cutting edge radius (r_n) was 0.044 ± 0.019 mm for the uncoated tool and 0.055 ± 0.023 mm for the coated tool.

The thermal conductivities of the uncoated and coated cutting inserts were found to be temperature depend. These dependencies are given in by the following equations [15]: (a) for the uncoated tool,
$$k_t(T) = 85.932 - 0.0057 \cdot T - 6 \times 10^{-5} \cdot T^2 + 4 \times 10^{-8} \cdot T^3$$
(W/mK); (b) for the coated tool,
$$k_t(T) = 25.86 + 0.0104 \cdot T - 3 \times 10^{-6} \cdot T^2 \text{ (W/mK)}.$$

Cutting regime parameters. The range of machining regimes used in the tests was selected using the data provided by the tool manufacturer for tool life of approximately 15 minutes. The range of the cutting speed was 75 – 200 m/min; that of the cutting feed was 0.05 – 0.10 mm/rev; that of the depth of cut was 2.5 – 5.0 mm. No cutting fluid was used in the tests.

4.2 Comparison of predicted and experimental results

The results obtained using the analytical approach represented by the flowchart shown in Figure 5 are shown in Figure 7 through Figure 10. Figure 7 and Figure 8 show the influence of RTS on the maximum temperatures at the tool-chip interface, T_M, and at the tool-workpiece interface, T_N, for the work materials and tools used in this study. These figures also shown the temperature at the chip free surface, T_{cf}, and the temperature at the chip contact surface, T_{cc}, measured using the above referred thermal imaging equipment.

According these figures, for the work materials and tools used in the cutting tests, T_M always increases with RTS while T_N tends to stabilize around a certain temperature level. For most RTS values, T_M is always higher than T_N.

However, for extremely low values of RTS, T_N becomes slightly higher than T_M. This can be explained by the reduction of the tool-chip contact length as the tool cutting edge radius increases (so, RTS decreases) [1]. In such conditions, the maximum cutting temperature zone shifts towards the tool flank. To verify the discussed results, FEM simulations of temperature distribution in the deformation zone of the equivalent orthogonal cutting model were carried out. Figure 11 [4] presents an example of the obtained results. As seen, when RTS is small, i.e. the radius of the cutting edge is great compare to the uncut chip thickness, the maximum temperature tends toward the flank.

Figure 7 and Figure 8 also show that the measured chip temperatures (T_{cc} and T_{cf}) are always higher than T_M (calculated), especially for extremely low values of RTS. However, the difference between the measured chip temperatures and T_M tends to decrease as RTS increases. Because the analytical approach considers only the cutting process taking place in the layer of thickness a_1 (Figure 1), the difference between the experimental and calculated temperatures is probably due to the ploughing phenomenon. Indeed, an increase in the cutting tool edge radius (or the corresponding decrease of RTS) increases ploughing, which competes directly with the cutting process.
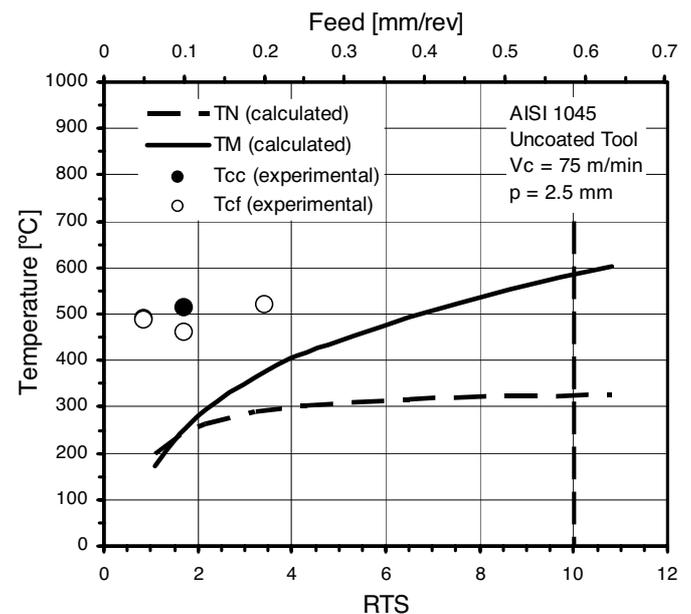

Figure 7: Influence of RTS on temperatures in cutting zone when machining AISI 1045 steel using the uncoated tool.
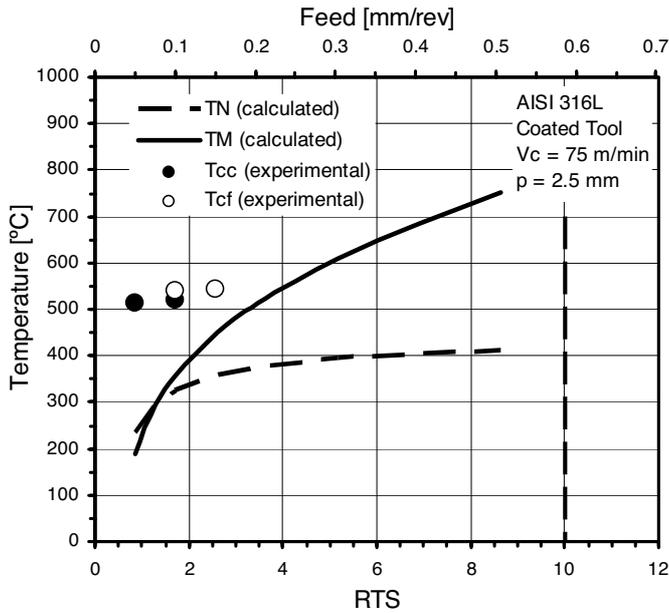
Figure 8: Influence of RTS on temperatures in cutting zone when machining AISI 316L steel using the coated tool.

As seen in Figure 9, there is the difference between the experimentally obtained and calculated temperatures over the range of the cutting speed used in the study, reinforcing the hypothesis that this difference can be attributed to the ploughing phenomenon.
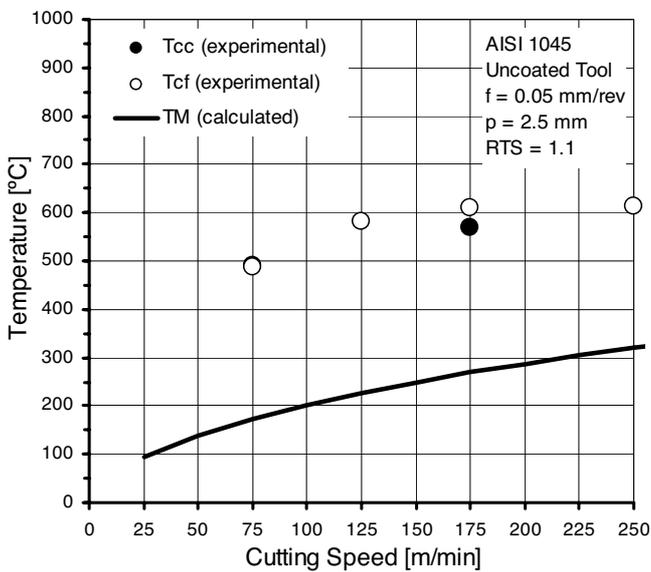

Figure 9: Influence of the cutting speed on temperatures in cutting zone when machining AISI 1045 steel using the uncoated tool.

The analytical approach presented in the previous section also allowed calculating the amount of thermal energy transported by the chip (Q_c), conducted into the workpiece (Q_w) and conducted into the tool (Q_t). Figure 10 shows the energy partition as a function of

RTS, for AISI 1045 steel when machined with the uncoated tools. As seen, the amount of heat conducted into the tool and into the workpiece increases as RTS decreases. Therefore, less heat is transported away from the cutting zone by the chip.
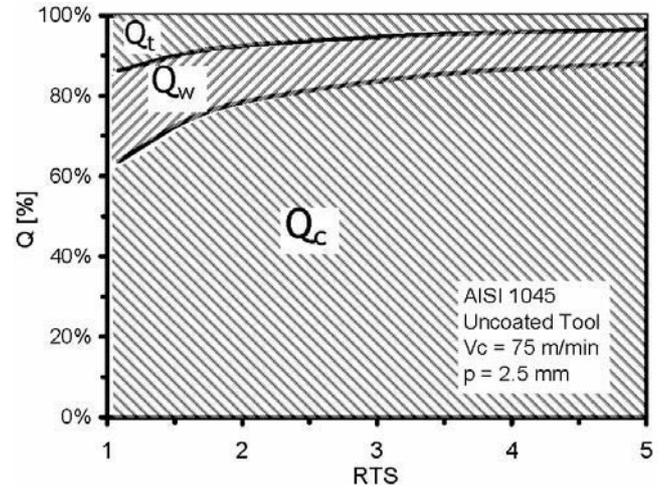

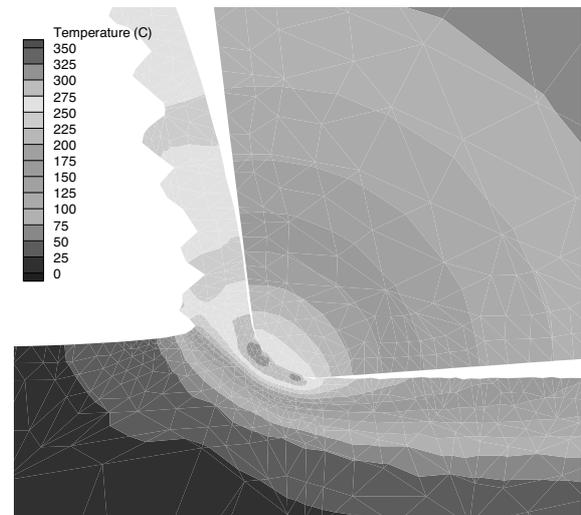Figure 10: Influence of RTS on energy balance when machining AISI 1045 steel using the uncoated tool.

Figure 11: Temperature distribution in the deformation zone in orthogonal cutting of the AISI 316L using the uncoated tool (RTS = 1.1) [4].

5 CONCLUSIONS

Being important parameter of the cutting tool, the tool sharpness cannot be defined as an absolute parameter characterized only by a particular value of the radius of the cutting edge. Rather, it is a relative parameter, which depends on both the radius cutting edge and the uncut chip thickness. It is proposed, therefore, to characterise tool sharpness by the Relative Tool Sharpness (RTS) defined as the ratio of the uncut chip thickness and the cutting

tool edge radius. To minimize the influence of the cutting tool edge radius in the cutting process, RTS should be kept higher that the critical relative tool sharpness $RTS_{critical}$. The establishment of this critical value will be objective of future developments and it should be made taking into account a physical rather than purely geometric approach.

For the same uncut total chip thickness, decreasing RTS leads to a decrease in the actual uncut chip thickness and to the corresponding increase in the thickness of the layer being burnished by the round part of the tool cutting edge due to ploughing. As a result, more heat generates in machining and a greater part of this heat is conducted into the tool and workpiece. As such, the portion of this heat transported away from the cutting zone by the chip decreases. Therefore RTS changes heat partition in the machining zone.

This change in heat partition directly affects temperature distribution in the deformation zone. The region of the maximum temperature shifts from the tool rake face to the tool flank face. This is particularly true for extremely low RTS'. When this is the case, the maximum temperature at the tool-workpiece interface (T_N) can be higher than that at the tool-chip interface (T_M).

The observed difference between the experimental and calculated temperatures is probably due to the ploughing phenomenon, because the analytical approach used in this study considers only the chip separation process and does not consider heat generated due to ploughing. This difference, however, decrease as the RTS parameter increase due to the reduction of the amount of heat generated due to ploughing.

6 REFERENCES

[1] N. N. Zorev, Metal Cutting Mechanics, Pergamon Press, Oxford, 1966.

[2] P. Albrecht, "New developments in the Theory of the Metal Cutting Process. Part I - The ploughing Process in Metal Cutting," Journal of Engineering for Industry 1960, 81, 348-358.

[3] P. K. Basuray, B. K. Misra, G. K. Lal, "Transition from Ploughing to Cutting during Machining with Blunt Tools," Wear 1977, 43, 341-349.

[4] J. C. Outeiro, "Application of Recent Metal Cutting Approaches to the Study of the Machining Residual Stresses (in Portuguese)," PhD Thesis, University of Coimbra 2002.

[5] J. A. Arsecularatne, P. Mathew, P. L. B. Oxley, "Prediction of Chip Flow Direction and Cutting Forces in Oblique Machining with Nose Radius Tools," Proceedings of the Institution of Mechanical Engineers, Part B: Journal of Engineering Manufacture 1995, 209, 305-315.

[6] J. Wang, P. Mathew, "Prediction of Chip Flow Direction and Cutting Forces in Oblique Machining with Nose Radius Tools. Report 1988/IE/5." University of New South Wales, Australia, 1988.

[7] J. Wang, P. Mathew, "Development of a General Tool Model for Turning Operations Based on a Variable Flow Stress Theory," International Journal of Machine Tools and Manufacture 1995, 35, 71-90.

[8] M. I. Klushin, Metal Cutting, Mashgiz, Moscow, Russia, 1958.

[9] V. P. Astakhov, Metal Cutting Mechanics, CRC Press, Boca Raton, USA, 1998.

[10] V. P. Astakhov, "Tribology of Metal Cutting," in Mechanical Tribology. Material Characterization and Application. G. Totten, H. Liang, Eds, Marcel Dekker, 2004 10-50.

[11] J. C. Outeiro, A. M. Dias, J. L. Lebrun, "Experimental Assessment of Temperature Distribution in Three-Dimensional Cutting Process," Machining Science and Technology 2004, 8, 357-376.

[12] R. J. Clifton, R. W. Klopp. Metals Handbook. 9th ed., edited by ASM. 1985.

[13] www.matweb.com.

[14] P. Lacombe, B. Baroux, G. Beranger. Les Aciers Inoxidables. edited. 1990, Les Editions de Physique: Les Ulis, França.

[15] I. S. Jawahir, C. A. Van Luttervelt, "Recent Developments in Chip Control Research and Applications," Annals of the CIRP 1993, 42, 659-693.